

Comment on ‘Banana–doughnut kernels and mantle tomography’ by van der Hilst and de Hoop

R. Montelli,* G. Nolet and F. A. Dahlen

Department of Geosciences, Princeton University, Princeton, NJ 08544, USA. E-mail: nolet@princeton.edu

E debbasi considerare come non è cosa più difficile a trattare, né più dubbia a riuscire, né più pericolosa a maneggiare, che farsi capo ad introdurre nuovi ordini. Perché lo introduttore ha per nimici tutti quelli che delli ordini vecchi fanno bene, et ha tepidi defensori tutti quelli che delli ordini nuovi farebbono bene.[†]

Machiavelli, *Il Principe*

Accepted 2006 September 4. Received 2006 May 31; in original form 2006 January 18

SUMMARY

The claim by van der Hilst and de Hoop that finite-frequency (FF) inversion of seismic traveltimes does not result in measurable improvements in tomographic images is misguided, and based upon a biased selection of images in the upper mantle, where wave front healing effects are indeed small, and where our models are generally poorly resolved because we primarily used teleseismic waves that travel steeply in the upper mantle; and upon an improper application of statistics to the better-resolved anomalies in the lower mantle. If station corrections for long-period *P* waves are computed using ray theory, as we do, unmodelled FF effects may be responsible for slow anomalies of up to 0.3 per cent beneath very small island stations, but these effects are negligible for larger islands such as Reunion and Kerguelen. The presence of a plume beneath these islands is the most probable explanation for the observed low velocities.

Key words: global seismology, plumes, sensitivity, tomography, traveltimes.

1 INTRODUCTION

van der Hilst & de Hoop (2005, hereafter referred to as HH) question whether finite-frequency (FF) sensitivity kernels (or banana-doughnut kernels, BDKs) enable significant improvements in the quality of whole-mantle tomographic images compared to seismic ray theory. Much of their discussion is devoted to a criticism of our own analysis of this important issue, published in Montelli *et al.* (2004b, hereafter M1). HH also compare the *P*-wave model published by Montelli *et al.* (2004a, hereafter M2) with the most recent MIT model MIT-P05 and conclude that the ‘better theory has not yet resulted in significant model improvements’. Even though they acknowledge that this ‘does not imply that the models based on BDKs are incorrect’, HH raise a number of doubts about the model published in M2. In this comment, we counter those arguments. As we discuss below, the model was in fact in need of a correc-

tion, but this correction does not affect any of the important conclusions about the existence of lower-mantle plumes, nor does it negate our earlier conclusions about the effectiveness of BDKs in mantle tomography.

We are grateful to the authors for complying with our request that they disconnect their model comparisons from an earlier exchange of viewpoints on theoretical questions in which Montelli had no part (Dahlen & Nolet 2005; de Hoop & van der Hilst 2005a,b), thus enabling us to respond properly in this comment. We are also grateful to van der Hilst for his analysis of the model published in M2, which prompted us to review our software extensively, leading to the discovery of an error in our ray theoretical (RT) crustal-correction algorithm, and thereby to improvements in subsequent tomographic models. An updated model of *P*-wave velocity heterogeneity, together with an independent *S*-wave velocity model, have recently been submitted for publication in *G*³ (Montelli *et al.* 2006). Both models, which we hereafter designate PRI-P05 and PRI-S05, provide strong support for the existence of lower-mantle plumes.

Dahlen *et al.* (2000) published an efficient method that corrects for wave front healing in cross-correlation traveltimes tomographic inversions. Following this theoretical development, we set out to test the effects of such ‘FF’ sensitivity kernels on a small data set of long-period *P* and *PP* waves that bottom beneath the transition zone. We focused our analysis on the lower mantle (the tomographic images in M1 start at 925 km depth) and restricted

*Now at: ExxonMobil Upstream Research Company, PO Box 2189, GW03-940A, Houston TX 77252-2189, USA.

[†]It must be considered that there is nothing more difficult to handle, more uncertain to succeed, nor more perilous to conduct, than to take the lead in the introduction of a new order of things. Because the innovator has for opponents all those who have done well under the old order, and lukewarm defenders among those who may do well under the new.

attention to long-period waves, because wave front healing effects are most pronounced in this case. Despite the obvious limitations in this data set, we made the serendipitous discovery of approximately one dozen lower-mantle plumes in our first global FF inversion attempts. This bolstered our hopes that the new inversion technique could lead to significant improvements in seismic tomography. We presented a detailed comparison of FF and RT inversions based upon *the same* long-period data, fitted at *the same* level of χ^2 , in M1. In our next inversions, we added short-period ISC *P* and *pP* data from Engdahl *et al.* (1998), to exploit what is probably the strongest suit of banana–doughnut theory: its ability to combine data observed at different frequencies, with different off-ray sensitivities, thereby providing extra leverage to constrain the size and magnitude of velocity anomalies. These results were published in M2.

2 UPPER VERSUS LOWER MANTLE

The most relevant result for the present discussion is fig. 9 in M1, which shows a number of low-velocity anomalies that exhibit a remarkable continuity with depth in the *lower* mantle, and which by virtue of their association with geologically identified hotspots, we identified as mantle plumes. Visual inspection of our maps shows that the amplitude of these lower-mantle plumes is almost always stronger in the model obtained using FF BDKs than in the corresponding RT model. HH present similar plume comparisons in their figs 2–5, but with one exception these are all located in the *upper* mantle. They conclude on the basis of their comparisons that ‘the effect of BDKs on both the pattern and the amplitude of wave speed perturbations appears to be smaller than that of practical (and sub-

jective) considerations (such as level of damping, the weighting of different data sets, and the choice of data fit)’. We do not wish to contest their conclusion as far as the upper mantle is concerned, since we did not include any long-period *pP*-wave or surface-wave data in our inversions, and that is where the BDKs of *P* and *PP* waves narrow down substantially and wave front healing effects are expected to be less pronounced. However, by asking readers to ‘visually inspect’ map images in the upper mantle, HH stop short of proving their point.

The one deep plume image shown by HH is Hawaii at 1350 km depth, which we exhibit in a larger whole-mantle context in Fig. 1. Hawaii is a poorly resolved plume in both models PRI-P05 and PRI-S05, but both the Princeton *P*- and *S*-wave images are in agreement that the plume splits up in the mid-mantle. The MIT-P05 image shows less detail and damps away in the lowermost part of the mantle. The improvement in spatial resolution is an expected consequence of FF theory, because the BDK sensitivity extends well beyond the rather narrow bundle of geometrical ray paths for the long-period data. It would be interesting to see if the disappearance of the plume in the MIT-P05 image could be remedied by relaxing the damping without violating χ^2 beyond reasonable limits and without blowing up the noise, but so far we see no reason to agree with HH that the FF theory employed in our inversions does not lead to better lower-mantle images.

The fig. 1 in HH also extends to the lower mantle, but it shows only selected cross-sections of the subducted Farallon and Antilles slabs. Such images have little bearing on the issue of the effectiveness of BDKs, since the laterally extensive character of slabs make them less prone to wave front healing than plumes. Unlike HH, we do not use a densified grid where one might expect to see subducted

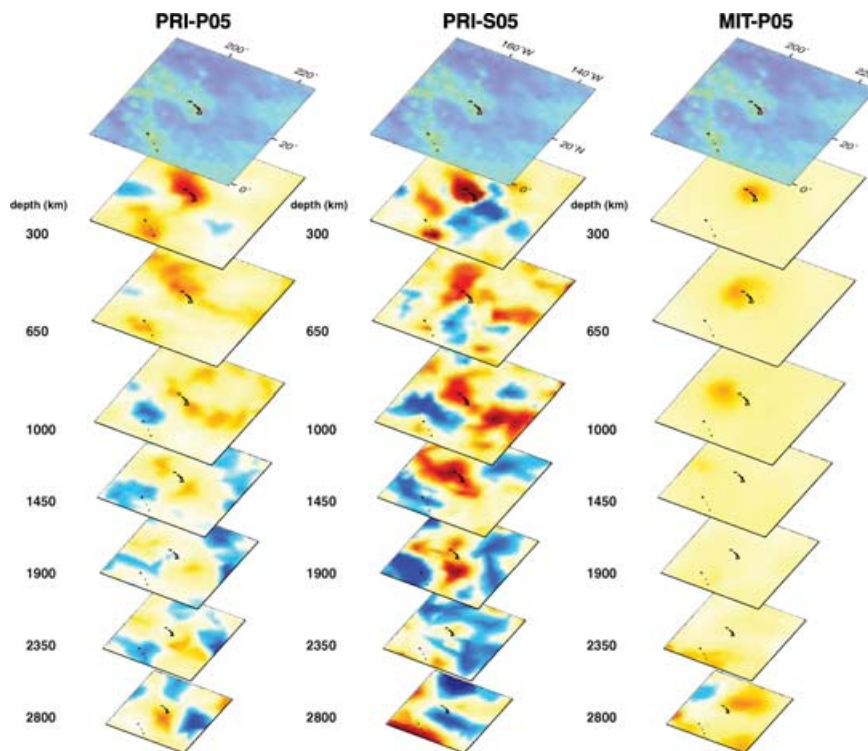


Figure 1. A comparison of images of the Hawaii plume in the tomographic models PRI-P05, PRI-S05 and MIT-P05 (from left to right). The full colour scale is ± 1.5 per cent for the two *P*-wave models and ± 3 per cent for the *S*-wave model PRI-S05. The splitting of the plume into two branches, visible in both PRI-P05 and PRI-S05, is perpendicular to the along-ray smearing in the northeast–southwest direction predicted by resolution tests. The splitting is not visible in model MIT-P05, which also seems to lose track of the plume at deeper levels, where Hawaii is particularly poorly resolved.

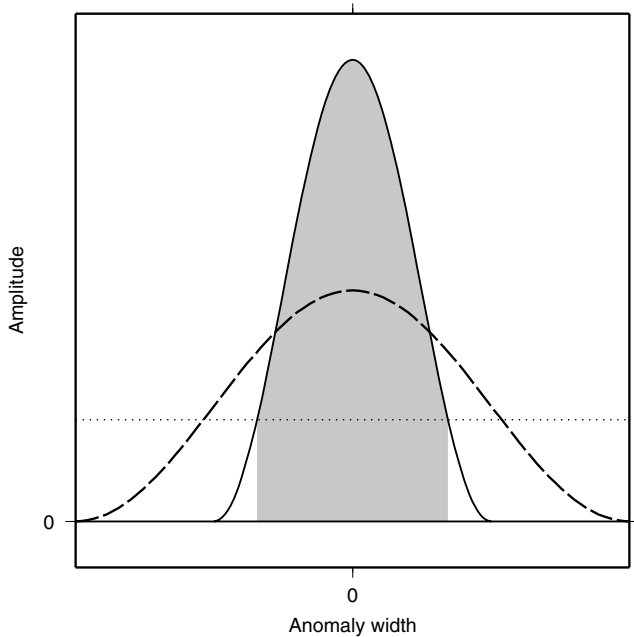


Figure 2. This cartoon illustrates why we feel that the statistical analysis of HH is flawed. The solid line shows a 1-D cross-section through a hypothetical velocity anomaly as correctly imaged using FF theory. When the healed traveltimes are inverted using ray theory, the anomaly is damped and widened, as shown schematically by the dashed line. M1 restricted attention to gridpoints lying above an amplitude threshold (dotted line) on the FF image, and compared the ratio between the two curves only within the grey interval; such a comparison measured the amplitude-enhancement effect of FF inversion at the location of the anomaly. HH include the tails of the RT anomaly, where the loss of signal at the centre of the anomaly is compensated by wave front healing, thus annihilating the statistical estimate of the magnitude of the beneficial effects of FF inversion.

slabs or their downdip extensions. Doing so might have improved our resolution for slabs, but would have been of little use in answering the limited question we had posed ourselves in M1: how strong is the effect of wave front healing on long-period tomographic inversions?

We also note that the comparisons in figs 1 and 2 of HH with the model published in M2 are meaningless, since this model was obtained by inverting a greatly expanded data set, including high-frequency ISC data from Engdahl *et al.* (1998). HH ignore the discussion in M2, where we speculate why the ISC data seem to require somewhat smaller anomalies for the same level of χ^2 (see also the discussion in Section 5 below). A comparison of the models in M1 and M2 is like comparing apples and oranges.

3 STATISTICAL ANALYSIS

M1 concluded that ‘depending on the depth and size of the anomaly, velocity perturbations in the FF tomographic images are 30–50 per cent larger than in the corresponding RT images’. This finding was based on a simple statistical analysis of histograms of the ratio $(\delta v_P/v_P)_{FF}/(\delta v_P/v_P)_{RT}$ between anomalies in the FF and RT images. An *anomaly* was defined for the purposes of this comparison as any model gridpoint where $|(\delta v_P/v_P)_{FF}| > 0.2$ per cent. We agree with HH that this amplitude threshold is somewhat arbitrary; we regret we did not provide the necessary arguments for such a threshold in M1, and we rectify this omission in the remainder of this section. We also note that $|(\delta v_P/v_P)_{FF}| > 0.2$ per cent is a con-

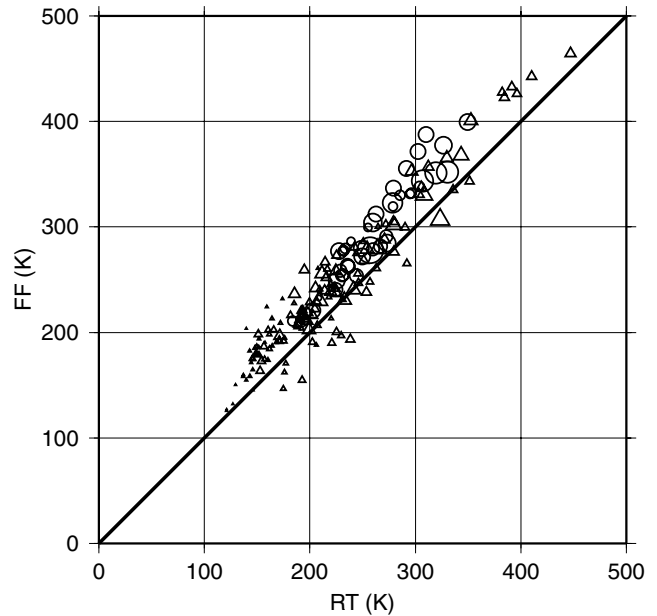


Figure 3. The inferred excess temperatures δT for shallow (<1000 km, triangles) and deep (1000–2000 km, circles) plumes show a clear depth dependence of the ratio between the FF and RT model values, and an average FF temperature enhancement of 13 per cent for the deeper plumes. The radius of the symbols is a qualitative indication of the plume size in the images shown in M1. The highest excess temperatures are within the transition zone and may reflect an underestimate of $\partial v_P/\partial T$. Note that the value of this partial derivative does not affect the temperature ratio $\delta T_{FF}/\delta T_{RT}$.

servative, low threshold: raising it to $|(\delta v_P/v_P)_{FF}| > 0.3$ per cent would increase the amplitude enhancement effects of FF inversion, which we were seeking to quantify in our M1 comparison.

In an effort to avoid a perceived bias, HH omit the threshold completely in their own statistical analysis. This approach ignores an essential characteristic of wave front healing. In a numerical study using the one-way wave equation, Nolet & Dahlen (2000) showed how healing leads to a spreading of the anomaly over a wider surface on the wave front. In this one-way approximation, traveltimes anomalies satisfy a diffusion equation, and what diffuses away from the centre of the wave front anomaly is added to a circular region around it. Dahlen (2004) investigated the effect of this on tomographic images, using a more accurate Radon transform analysis, and showed that in the highly idealized case of perfect geographical coverage, the volume integrals over an isolated FF and RT model anomaly are identical. This implies that away from the actual anomaly, the ratio $(\delta v_P/v_P)_{FF}/(\delta v_P/v_P)_{RT}$ necessarily becomes smaller than one, as illustrated schematically in Fig. 2. Including these small values in an analysis of the ratio $(\delta v_P/v_P)_{FF}/(\delta v_P/v_P)_{RT}$, as HH do, leads predictably to a null result, that is, a histogram centred on a ratio near unity.

To explore this aspect a little further, we focus upon the amplitude enhancement of the imaged plumes in particular. Fig. 3 compares the inferred maximum temperature anomalies at the centres of the plumes listed in table 1 of M2, at depths between 300 and 2000 km in the RT versus FF tomography models derived in M1 (we compare maxima even if these are at different locations in the two models). Using temperature rather than P -wave velocity as a basis of comparison has the advantage of eliminating the effect of decreasing $\partial v_P/\partial T$ with depth on the value of $\delta v_P/v_P$. Selecting plume anomalies also removes the bias introduced in M1 by

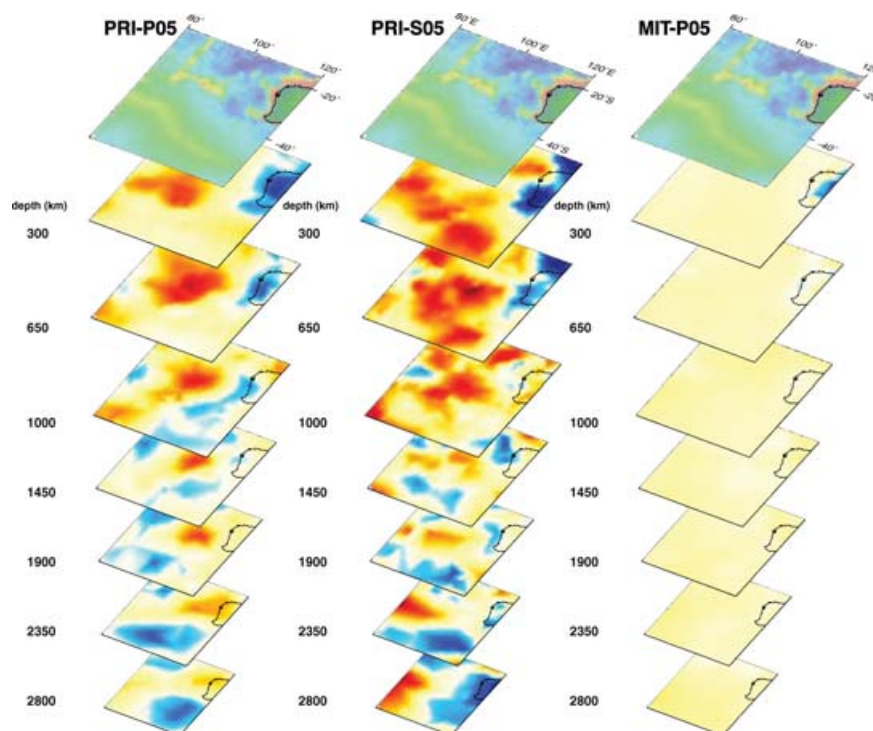


Figure 4. Same as Fig. 1, but for the Indian Ocean plume. Note the absence of a clear plume signal in model MIT-P05 (right), which is based upon a similar short-period data set as used for PRI-P05 (left) but lacks the long-period data interpreted with FF theory that helped constrain the plume in PRI-P05 and PRI-S05 (centre). See text for further discussion.

identifying anomalies from the FF model only (though because of the amplifying effect of FF, this bias was actually small). On average, the FF temperature anomalies of plumes are 9 per cent higher at depths less than 1000 km and 13 per cent higher at depths between 1000 and 2000 km, with the largest enhancements near 30 per cent. This is less than the ‘30–50 per cent’ velocity enhancement quoted in M1 and contested by HH, largely because the spatial extent of these well-resolved plumes is larger than the smallest anomalies that dominate in the M1 point-by-point analysis. It is perhaps this aspect of our statistical analysis that gave rise to the present discussion, and we are glad to be able to clarify this misunderstanding.

4 CRUSTAL CORRECTIONS

Some of the differences between models PRI-P05 and MIT-P05 in the upper mantle have little to do with the issue of FF versus RT inversions, in as much as the two models have been obtained using different data, fit at different (and in the MIT case unstated) levels of χ^2 , different damping schemes, and in all likelihood a different zero level for the background spherically symmetric model. Nevertheless, these upper-mantle differences prompted us to review our procedure for making crustal corrections, which led to the discovery of an error (the faulty computer code produced an error having a different sign depending on whether the local crustal thickness in model CRUST2.0 is larger or smaller than the spherically averaged crust in model *iasp91*). This crustal-correction error did have some influence on the published images, especially at shallow depths, but it in no way affects the conclusion by M2 that a significant number of plumes originate in the lower mantle. Since the error is the same for the FF and RT inversions it also does not affect the FF–RT comparisons made in M1.

HH assert on the basis of their fig. 5 that ‘plume signatures show up only below the ocean island stations that contribute to the set of long-period data’. This statement is not correct: for example, we see a plume under Bouvet Island and another under the East Indian Ridge (see Fig. 4), where no seismic stations—either short-period or long-period—are even nearby. However, the poor agreement between models PRI-P05 and MIT-P05 beneath islands such as Reunion and Kerguelen (see Fig. 5) prompted us to investigate the legitimate question whether our RT station corrections might be insufficient: if the actual wavefield suffers from FF effects and is slowed down by the adjacent water layer, a crustal correction computed using ray theory would predict an arrival that is too early, and a spurious low-velocity anomaly, streaked along well-sampled ray directions in the upper mantle, would result. To investigate possible FF effects for island station corrections, we performed a simplified, 2-D finite-difference computation in which a plane wave front impinges from a vertical direction on a 20-km-wide island in a 5.6-km-deep ocean. The observed broad-band pulse was filtered and cross-correlated with a realistic source time function. When high-pass filtered to mimic a short-period seismometer, the arrival is 0.03 s faster than predicted by ray theory; a bandpassed long-period pulse (0.015–0.07 Hz) arrives 0.20 s later. If we spread this FF effect over the depth of the upper mantle, the associated velocity anomaly is $\delta v_P/v_P = -0.3$ per cent. This is a worst-case scenario, because the adopted island width of 20 km is much smaller than the typical 50 km width of islands such as Reunion or Kerguelen; the corresponding long-period FF–RT time difference for a 50-km-wide island is only 0.05 s. The observed upper-mantle plume anomalies beneath Reunion and Kerguelen in model PRI-P05 are $\delta v_P/v_P = 1$ –2 per cent; thus, these anomalies cannot be attributed to unmodelled FF crustal effects. A fuller study, using 3-D rather than 2-D geometry, a more realistic geography of the islands, and actual

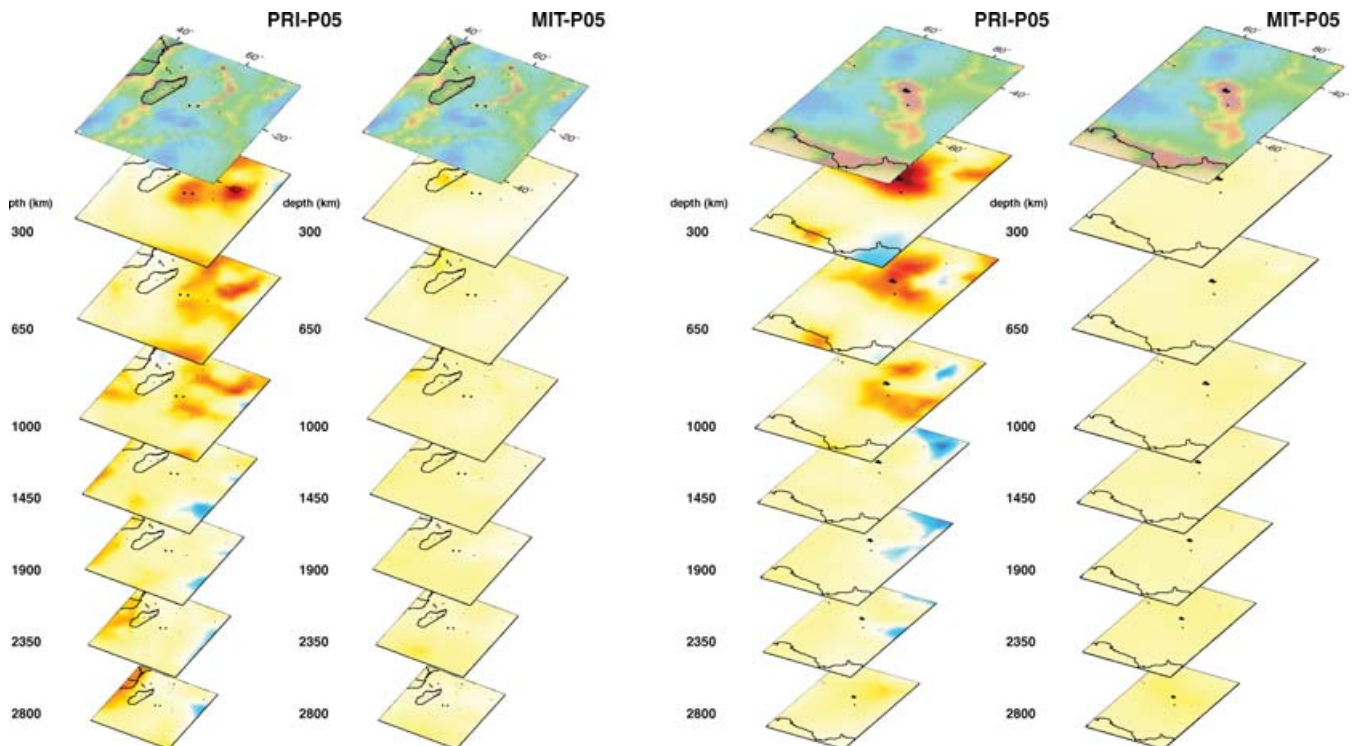


Figure 5. From left to right: the mantle images beneath Reunion in model PRI-P05 and MIT-P05 and beneath Kerguelen in PRI-P05 and MIT-P05. The colour scale extends from -1.5 to 1.5 per cent. In the text, we argue that the presence of plumes beneath Reunion and Kerguelen in the Princeton model cannot be attributed to unmodeled FF effects in the crustal corrections of long-period arrival times. Compare with Fig. 4, which lacks any island station near the plume.

station locations would be needed to give a more precise estimate for the smallest oceanic island stations, but the effect seems unlikely to be large enough to explain more than a small fraction of any observed plume anomaly.

5 CHI-SQUARED

In their discussion, HH contend that the significance of differences between FF and RT inversions are smaller than the ‘effects of data errors and practical (and subjective) considerations such as ... the choice of data fit (the value of χ^2)’. They also question our use of assigned ‘data errors well below 1 s’. The only argument put forward for the disagreement with our error estimates is the fact that the average of our long-period data is offset by about 5 s from the average of the ISC data. This offset of several seconds is to be expected, because a long-period, cross-correlation measurement centres on the traveltime of the maximum energy in a pulse, rather than on a possibly small initial onset. Thus, so-called ‘centroid’ origin times are likely to be later than those listed in short-period catalogues, and the magnitude of such an offset is in no way an indication of the observational error in the cross-correlation measurements. That the distinction between the long-period and short-period origin times is the cause of the offset is also supported by the absence of any offset observed for the differential data $pP-P$ and $PP-P$, and by the observation that the offset for individual events increases with seismic moment (G. Masters, personal communication, 2005). It was precisely for this reason that we allowed for different origin-time corrections for the short- and long-period data in M2.

The standard errors adopted for the long-period data are based upon the estimates made by the seismologists who performed the cross-correlation measurements (Bolton & Masters 2001): 0.44–

0.79 s for absolute P traveltimes and 0.75–1.15 for $PP-P$ residuals. The Cramér-Rao lower bound (Carter 1987) for the error in a cross-correlation arrival time is 0.35 s, assuming a signal-to-noise ratio greater than one, a bandwidth of 0.05 Hz and a window length of 20 s, so our error estimates are well within the expected range. The magnitude of the error does not really influence the conclusions of M1—who consistently compared models at the same value of χ^2 for the same data set—but could of course be used to challenge the importance of the FF versus RT effects, as HH do.

The error estimates we used in M2 for the short-period ISC data from Engdahl *et al.* (1998) are more uncertain. Error estimates for ISC data were first given by Morelli & Dziewonski (1987), who suggest an overall standard error for P waves of $\sigma_P = 1.4$ s. This estimate includes arrivals in a somewhat larger epicentral distance range than used in our study, and may be an overestimate also because of the rather wide ray bundles used. Gudmundsson *et al.* (1990), who took the width of ray bundles into account explicitly in the analysis, estimate the random errors in ISC data for our range of interest to be 1.0 s. The culling by Engdahl *et al.* (1998) is likely to have improved the precision, and a standard deviation of 0.9 s for P and 1.1 s for pP seemed reasonable to us.

As we discussed in M2, even though the ISC and long-period data can be inverted jointly to fit their separate expected χ^2 levels, the short-period data consistently predict lower-amplitude plume anomalies than the long-period data. To some degree, FF effects may even have influenced the short-period data. However, it seems more likely that the standard deviation of 0.9 s adopted in M2 is too pessimistic. In our recently submitted G^3 paper (Montelli *et al.* 2006) we obtain good agreement between the two frequency bands after lowering σ_P for the ISC data further to 0.7 s.

We agree with HH that there are uncertainties in the estimates of standard errors, but any such uncertainty needs to be weighed against its influence on χ^2 before a bland statement can be made that the beneficial effects of FF BDKs drown in the noise. It is a simple matter to make a back-of-the-envelope calculation based upon the trade-off curves in fig. 7 of M1. We would need to raise χ^2 for the FF model by 15 per cent to bring the amplitudes *on average* down to the level of the RT model. This would indeed be equivalent to a small adjustment of the assigned standard errors; however, as M1 argued, and as the analysis in HH confirmed, the *average* difference between our FF and RT models is not large: the difference in norm is mostly due to differences in the smaller-scale anomalies. The analysis in M1 showed that such local anomalies can differ in amplitude by as much as 50 per cent. To equalize the FF and RT amplitude of these small-scale anomalies, we would have to increase χ^2 by a similar percentage in the FF inversion. Only if one is darkly pessimistic about standard errors (e.g. if one fears that the culling of ISC data by Engdahl *et al.* (1998) has actually degraded the precision) can one argue that such a large uncertainty is warranted. The standard statistical measure of misfit, χ^2 , is often ignored by the tomographic community in favour of the meaningless ‘variance reduction’—reduced with respect to *what*? However, χ^2 is too good a statistic to be treated with disrespect, certainly if the errors are normally distributed (which one obtains at least approximately through the rejection of outliers and which in any case is consistent with the use of the criterion of least-squares in most if not all large tomographic inversions). See the discussion of this issue in M1.

6 LOWER-MANTLE PLUMES

In M2, we concluded that ‘culling of the highest quality short-period data and remeasurement of the long-period data, *in addition* to the implementation of FF sensitivity kernels and an irregular model parametrization’ led to the successful imaging of lower-mantle plumes. HH focus their criticism upon the FF method and conclude that the effect of BDKs on plume images has been overstated, which seems an inappropriate rendition of our writing; nevertheless, we stand by our view that the use of FF kernels was an important ingredient. In fact our most recent tomographic experiment reinforces that view: we have inverted long-period *S* waves without the benefit of a second frequency band. These results have been submitted elsewhere (Montelli *et al.* 2006), but Figs 1 and 4 show examples, compared to model MIT-P05. The complete absence of a plume under the Indian Ridge is especially striking in model MIT-P05 when compared to PRI-P05 and our virtually identical image of the Indian Ocean plume in the appendix of M2. This is a poorly resolved plume, but neither the model parametrization with randomly distributed interpolation supports, nor the regularization using isotropic smoothing, are favouring the pronounced vertical continuity that is visible, especially in the *P*-wave image. Moreover, we used no data from *PcP* or core phases, and the dominant *P* ray direction in the lower mantle is close to horizontal. As noted before, this plume is not capped by an island seismic station, as is the case with Reunion or Kerguelen. The columnar character of the Indian Ocean plume is thus without any doubt a characteristic that is present in the data, and not an artefact of the inversion. Given the overlap in short-period data between models PRI-P05 and MIT-P05, our inversion of the long-period data using FF BDKs is the main factor distinguishing the two models.

The *S*-wave tomography confirms the lower-mantle plumes first published in M2, but it also shows that the combination of two fre-

quency bands was a strong factor in the imaging of plumes. This factor was not tested in M1, and in fact we used ray theory for the short-period data in M2—both for lack of computational resources and because we felt that FF effects should be minor for these data given the length scales that we inverted for. Clear evidence for FF traveltime dispersion has recently been observed by Sigloch & Nolet (2006), providing a direct data-space indication that the earth contains heterogeneities at length scales sensitive to wave front healing. Exploiting the frequency dependence of traveltime sensitivity seems to us at this stage to be more productive than prolonging the debate about the efficacy of FF theory. The superiority of FF theory for body waves had been demonstrated in a series of papers using synthetic data (Hung *et al.* 2000, 2001; Baig *et al.* 2003; Baig & Dahlen 2004) before being tested on a real-world tomographic application in M1 (and for surface waves by Zhou *et al.* 2004; Yang & Forsyth 2006). If HH or other seismic tomographers are still convinced that BDKs have no beneficial effects, we challenge them to produce high-quality lower-mantle plume images using ray theory.

ACKNOWLEDGMENTS

We thank Rob van der Hilst for his critical analysis of the models in M1 and M2. His comments led to the discovery of an error in our RT crustal-correction procedure which has been remedied in model PRI-P05. We also thank Rob for making model MIT-P05 available to us for comparisons. We gratefully acknowledge support for the development of FF tomography over the past decade at Princeton by various grants from the NSF Earth Sciences Program to GN and FAD.

REFERENCES

- Baig, A.M., Dahlen, F.A. & Hung, S.-H., 2003. Traveltimes of waves in three-dimensional random media, *Geophys. J. Int.*, **153**, 467–482.
- Baig, A.M. & Dahlen, F.A., 2004. Statistics of traveltimes and amplitudes in random 3-D media, *Geophys. J. Int.*, **158**, 922–938.
- Bolton, H. & Masters, G., 2001. Travel times of *P* and *S* from global digital seismic networks: implication for the relative variation of *P* and *S* velocity in the mantle, *J. geophys. Res.*, **103**, 13 527–13 540.
- Carter, G., 1987. Coherence and time delay estimation, *Proc. IEEE*, **75**, 236–255.
- Dahlen, F.A., Hung, S.-H. & Nolet, G., 2000. Fréchet kernels for finite-frequency travel times—I. Theory, *Geophys. J. Int.*, **141**, 157–174.
- Dahlen, F.A. & Nolet, G., 2005. Comment on ‘On sensitivity kernels for wave equation transmission tomography by de Hoop and van der Hilst’, *Geophys. J. Int.*, **163**, 949–951.
- Dahlen, F.A., 2004. Resolution limit of traveltime tomography, *Geophys. J. Int.*, **157**, 315–331.
- de Hoop, M.V. & van der Hilst, R.D., 2005a. On sensitivity kernels for ‘wave equation’ transmission tomography, *Geophys. J. Int.*, **160**, 621–633.
- de Hoop, M.V. & van der Hilst, R.D., 2005b. Reply to comment by F. A. Dahlen and G. Nolet on ‘On sensitivity kernels for ‘wave-equation’ transmission tomography’, *Geophys. J. Int.*, **163**, 952–955.
- Engdahl, E., van der Hilst, R.D. & Buland, R., 1998. Global teleseismic earthquake relocation with improved travel times and procedures for depth determination, *Bull. seism. Soc. Am.*, **88**, 722–743.
- Gudmundsson, O., Davies, J.H. & Clayton, R.W., 1990. Stochastic analysis of global travel time data: mantle heterogeneity and random errors in the ISC data, *Geophys. J. Int.*, **102**, 25–44.
- Hung, S.-H., Dahlen, F. & Nolet, G., 2000. Fréchet kernels for finite-frequency travel times – II. Examples, *Geophys. J. Int.*, **141**, 175–203.
- Hung, S.-H., Dahlen, F. & Nolet, G., 2001. Wavefront healing: a banana-doughnut perspective, *Geophys. J. Int.*, **146**, 289–312.

- Montelli, R., Nolet, G., Dahlen, F.A., Masters, G., Engdahl, E. & Hung, S.-H., 2004a. Finite-frequency tomography reveals a variety of plumes in the mantle, *Science*, **303**, 338–343.
- Montelli, R., Nolet, G., Masters, G., Dahlen, F.A. & Hung, S.-H., 2004b. Global *P* and *PP* traveltimes tomography: rays versus waves, *Geophys. J. Int.*, **158**, 637–654.
- Montelli, R., Nolet, G., Dahlen, F.A. & Masters, G., 2006. A catalogue of deep mantle plumes: new results from finite-frequency tomography, *Geochem., Geophys., Geosystems*, in press.
- Morelli, A. & Dziewonski, A.M., 1987. Topography of the core-mantle boundary and lateral homogeneity of the liquid core, *Nature*, **325**, 678–683.
- Nolet, G. & Dahlen, F.A., 2000. Wave front healing and the evolution of seismic delay times, *J. geophys. Res.*, **105**, 19 043–19 054.
- Sigloch, K. & Nolet, G., 2006. Measuring finite-frequency body wave amplitudes and traveltimes, *Geophys. J. Int.*, **167**, 281–287.
- van der Hilst, R.D. & de Hoop, M.V., 2005. Banana–doughnut kernels and mantle tomography, *Geophys. J. Int.*, **163**, 956–961.
- Yang, Y. & Forsyth, D., 2006. Regional tomographic inversion of the amplitude and phase of Rayleigh waves with 2-D sensitivity kernels, *Geophys. J. Int.*, **166**, 1148–1160.
- Zhou, Y., Dahlen, F. & Nolet, G., 2004. Three-dimensional sensitivity kernels for surface wave observables, *Geophys. J. Int.*, **158**, 142–168.